Crystallization, Tensile, and Impact Behavior of Polypropylene/Polybutadiene Blend

A. K. GUPTA and B. K. RATNAM

Centre for Materials Science & Technology, Indian Institute of Technology, New Delhi 110016, India

SYNOPSIS

A blend of isotactic polypropylene (PP) and polybutadiene (PBu), in the composition range 5–35 wt % PBu content, prepared by mixing in a two-roll mill, is studied for crystallization, tensile, and impact behavior. Variations in crystallization behavior and the resulting morphology and structure are observed in both differential scanning calorimetry (DSC) and X-ray diffraction measurements on this blend as a function of blend composition. Impact and tensile properties are studied in the entire blend composition range. Analysis of tensile properties data in terms of the various theoretical models is attempted to obtain better insight into the interphase adhesion and stress concentration effect in this blend. The effects of blend composition on the state of dispersion and morphology of dispersed phase droplets and correlation of tensile properties with the crystallization parameters of PP component are also presented.

INTRODUCTION

Isotactic polypropylene (PP) is a widely used thermoplastic. Efforts are being made to widen its scope of applications by blending with other polymers. Studies on the blends of PP with various elastomers[1-17] have shown improvements in not only the impact resistance but also the melt flow behavior related to processability and crystallization of PP. The studies on PP/elastomer blends, however, are mostly confined to using the elastomers—styrene–ethylene butylene–styrene triblock copolymer (SEBS),[1-6] copolymer of ethylene–propylene–diene monomer (EPDM),[7-11] and ethylene–propylene rubber (EPR).[12-17] A simpler and also less expensive elastomer, viz. polybutadiene (PBu), is rarely chosen for studies on blends with PP. In the present work, we undertake a study on the blend of PP with PBu. The PP/polybutadiene blend, in the composition range of 5–35 wt % polybutadiene content, is studied for its crystallization behavior, tensile properties, and impact resistance. Crystallization behavior is studied by differential scanning calorimetry (DSC) and X-ray diffraction measurements to examine the changes in structure and morphology with blending ratio. Furthermore, in addition to reporting the results about tensile and impact properties of PP/PBu blend in the studied range of blend composition, analysis of tensile data in terms of theoretical models is presented to reveal the effect of blend morphology and shape of dispersed phase droplets. Scanning electron microscopy is used to study the state of dispersion. A correlation of crystallinity and crystallite size distribution with mechanical properties is also presented.

EXPERIMENTAL

Materials

Polymers used were isotatic polypropylene of injection molding grade (Koylene grade-M-3030 of melt flow index 3.0, produced by Indian Petrochemicals Corporation Ltd.) and polybutadiene, molecular weight 2×10^5 as determined by viscosity measurements (produced by Synthetics and Chemicals Ltd.).

Binary blends of PP and PBu of varying blending ratios were prepared by mixing in a two-roll mill at 160°C. The PBu was cut into small pieces of size comparable to that of the PP granules to obtain a more uniform mixing in lesser time. Thus, a good

Journal of Applied Polymer Science, Vol. 42, 297–315 (1991)
 CCC 0021-8995/91/020297-19$04.00

mixing was achieved without any loss of whiteness of the mixed sample. The sheet obtained after mixing on the roll mill was cut into thin strips that were then passed through a granulator to obtain fine granules suitable for molding of the test specimens. The test specimens were cut out of the compression-molded sheets.

Measurements

Izod impact strength was measured on notched specimens on an FIE (model 042) impact tester. Rectangular specimens of dimensions 5 cm × 1 cm and thickness 0.3 cm with 2-mm-deep triangular notches of 45° were used.

Tensile properties were measured on an Instron Universal testing machine (Model 1121) at an elongation rate of 1 cm/min with an initial gauge length of 5 cm. Specimens used were dumbbell shaped with dimensions of 10 × 0.85 cm and thickness of 0.3 cm at the center.

DSC measurements were undertaken on a Dupont 990 thermal analyzer using the specimen (size 10 mg) in the form of powder (sawdust of the compression-molded sheet). In the DSC cell, the sample was first heated to 200°C (i.e., above the melting point of PP) and then, after a few minutes, the cooling cycle and the recording of thermogram was commenced at a cooling rate of 10°C/min.

X-ray diffraction patterns of powdered samples were recorded on a Philips Norelco X-ray diffractometer, in the 2Θ range from 8–40°C, using CuK_α radiation at scan speed 0.05°/sec.

Scanning electron micrographs (SEMs) of impact-fractured samples were taken on a Cambridge Instruments Scanning Electron Microscope (Model 54-10). Samples were etched with xylene at ambient temperature to dissolve the PBu phase.

RESULTS AND DISCUSSIONS

Crystallization Behavior

The crystallization of PP in the PP/PBu blend showed distinct dependence on the PBu content, as seen in both X-ray diffraction and DSC crystallization exotherm measurements. DSC thermograms in the region of crystallization, recorded during the cooling cycle, are shown in Figure 1. All thermo-

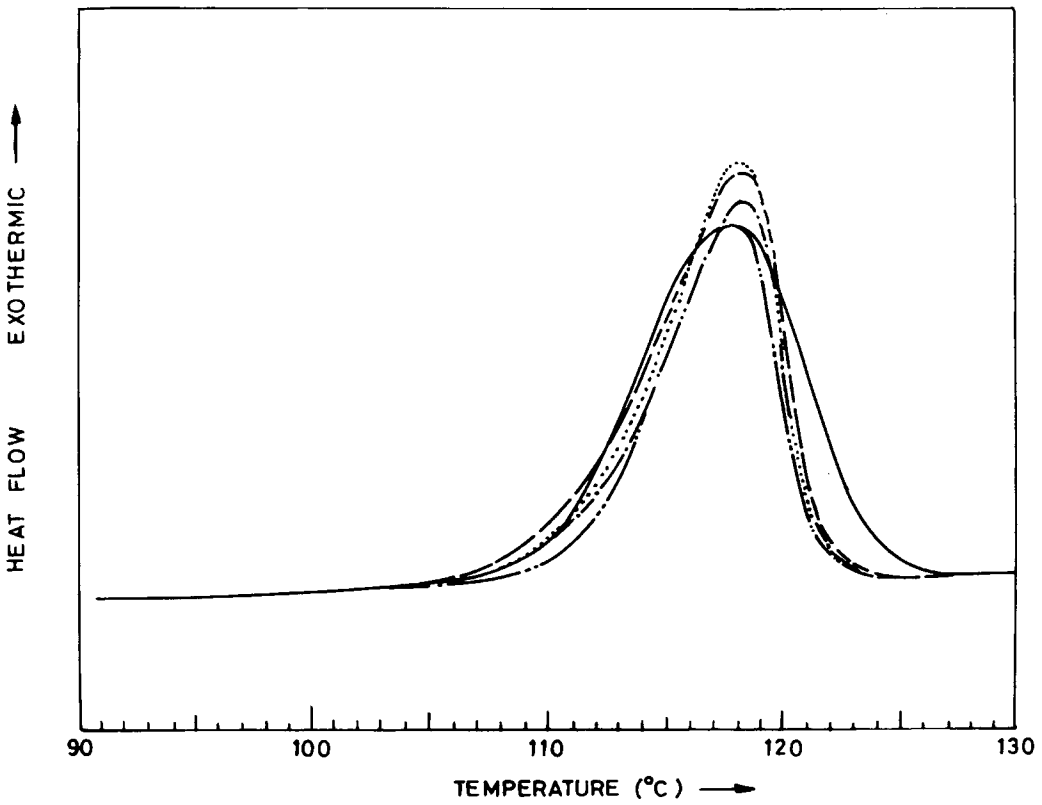

Figure 1 DSC exotherms representing crystallization of PP in PP/PBu blend at various PBU contents (wt %): —, 0; —, 5; · · · · · ·, 15; — · —, 25; — · · —, 35.

grams shown in the figure were recorded at identical experimental settings and almost equal sample weight; hence, they enable a good comparison in their shapes and locations on temperature scales. An analysis of these thermograms is done in terms of the five parameters defined below and shown in Figure 2.

T_p: Exotherm peak temperature.

S_i: Slope of initial portion of the exotherm. This slope is essentially influenced by the initial process of crystallization, viz. the nucleation. The faster the nucleation, the greater will be the initial slope.

T_{onset}: Temperature at onset of crystallization, which is the temperature where the thermogram curve departs from the baseline at the beginning of the exotherm.

Δw: Width at half-height of the peak. This is related to the distribution of crystallite size; the narrower the crystallite size distribution, the smaller will be the Δw.

A/m: Area under the exotherm per unit weight of the crystallizable component of the sample, which is proportional to the degree of crystallization.

This five-parameter model of analysis, used previously,[2,18] provides information on not only the crystallization parameters but also the morphology of the crystalline phase developed. However, this analysis is semi-quantitative, and its essential requirement is that the exotherms be recorded under identical conditions of experimental settings. The self-consistency of this analysis is inherent in the observation that an increase of S_i should be accompanied by a decrease in Δw (or vice versa) because faster nucleation results in almost simultaneous creation of most crystallites that subsequently grow to form a more uniform crystallite size distribution, whereas slow nucleation does not.

Plots of T_p, S_i, T_{onset}, Δw, and A/m as a function of blend composition are shown in Figure 3. It is seen that the addition of PBu produces a general increase of A/m, T_p, and S_i and decrease of Δw and T_{onset}. In addition to these general trends, there are distinct maxima or minima around 5 wt % PBu content in the variations of all these parameters.

On initial addition of 5 wt % PBu, the T_p shows a very small increase, while the T_{onset} decreases and at higher blending ratios both T_p and T_{onset} level off to constant values or show very slight variations. The initial slope, S_i, is higher for the blend than for the unblended PP, which is accompanied by a de-

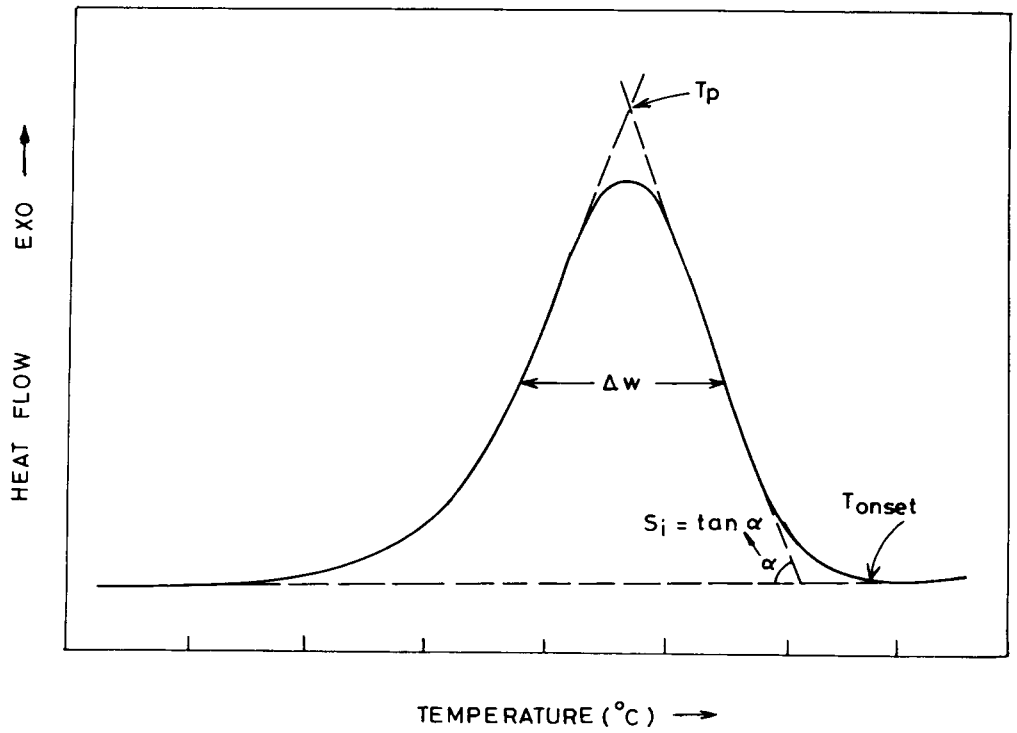

Figure 2 Typical crystallization exotherm, recorded during coding cycle, and the illustration of the various parameters used in the analysis.

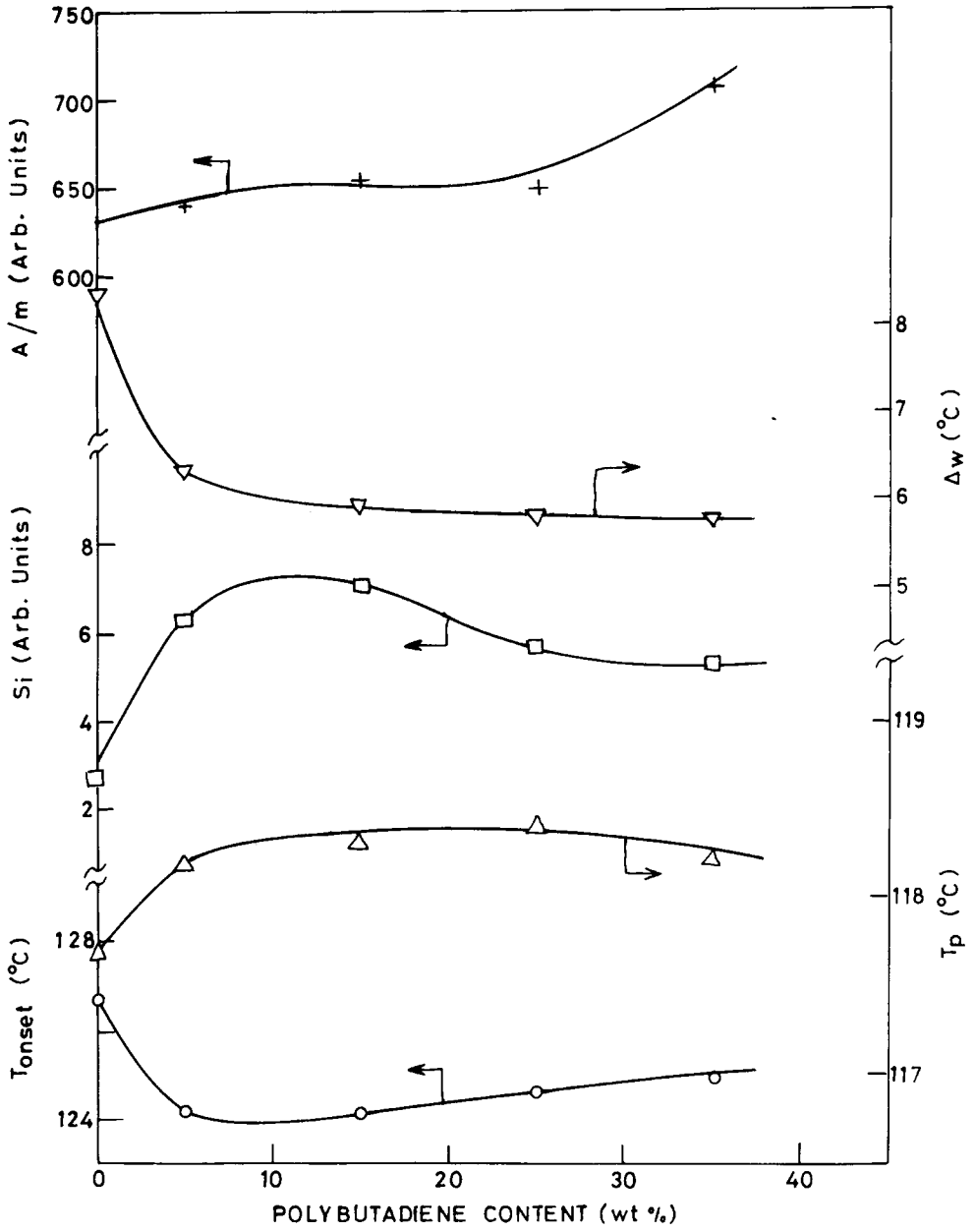

Figure 3 Variations of crystallization exotherm parameters T_{onset}, T_p, S_i, Δw, and A/m with PBu content for PP/PBu blend.

crease in Δw. The increase of S_i implies a faster rate of nucleation, which produces more uniformity of spherulite size, supported by the lower value of Δw implying narrower distribution of crystallite size. The ratio A/m increases quite inappreciably to 25 wt % PBu and thereafter rapidly with increase in PBu content of the blend.

Thus, from these variations in the DSC crystallization exotherms, crystalline morphology is clearly distinguishable in the two regions of the blend composition. In the first region, i.e., above 5 wt % PBu content, the rate of nucleation is fast; hence, the crystallite size distribution decreases. This gives rise to a morphology with a larger number of small (and of uniform size) crystallites. In the second region, i.e., at lower PBu content (<5 wt %), the S_i is small and Δw is large, which suggests a morphology with coexistence of small and large crystallites.

X-ray Diffraction

X-ray diffractograms for the various samples are shown in Figure 4. The characteristic diffraction maxima of monoclinic α-crystalline form[19] of PP

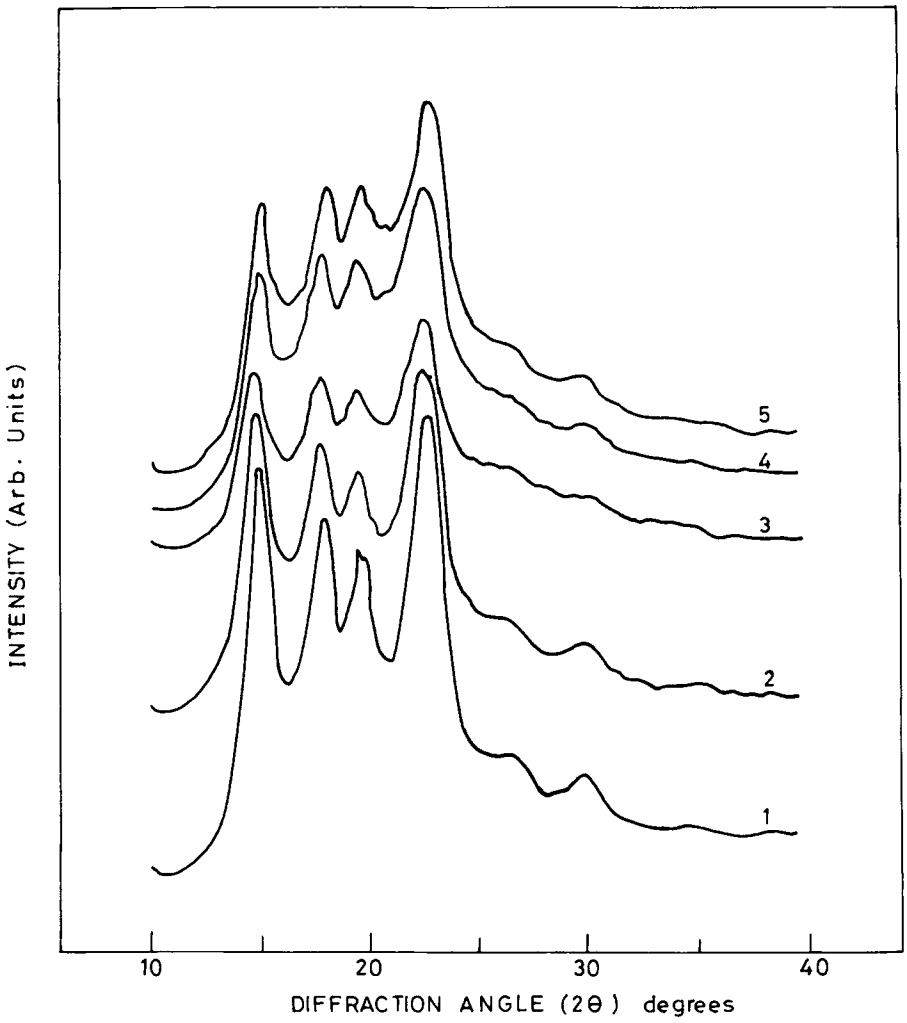

Figure 4 X-ray diffractograms of PP/PBu blend at various PBu contents (wt %): (1), 0; (2), 5; (3), 15; (4), 25; (5), 35.

(viz. the four intense peaks at 2Θ = 15, 17.8, 19.6, and 22.6°) are present in the diffraction patterns of all the samples of PP/PBu blend without any additional crystalline peak. However, a variation of background intensity with increasing PBu content, which might be an effect of amorphous scattering of PBu, is seen in these diffraction patterns. Changes in diffraction pattern with blend composition are quite systematic in terms of crystallinity, crystallite size, and the relative intensities of the diffraction maxima. The degree of crystallinity of the blend calculated from these diffraction patterns, as per the procedure used previously,[2] shown in Table I, decreases with increasing PBu content. Crystallinity

Table I Values of Various Parameters Determined from X-ray Diffraction

PBu Content (wt %)	Degree of Crystallinity (%)	Crystallite Size t_{110} (Å)	Crystallite Size t_{040} (Å)	Intensity Ratio I_{040}/I_{110}	Crystallite Size Ratio t_{040}/t_{110}
0	70.3	198	354	0.87	1.79
5	78.1	176	412	0.89	2.34
15	77.8	169	349	0.97	2.10
25	73.3	199	425	1.06	2.14
35	71.4	187	425	1.06	2.30

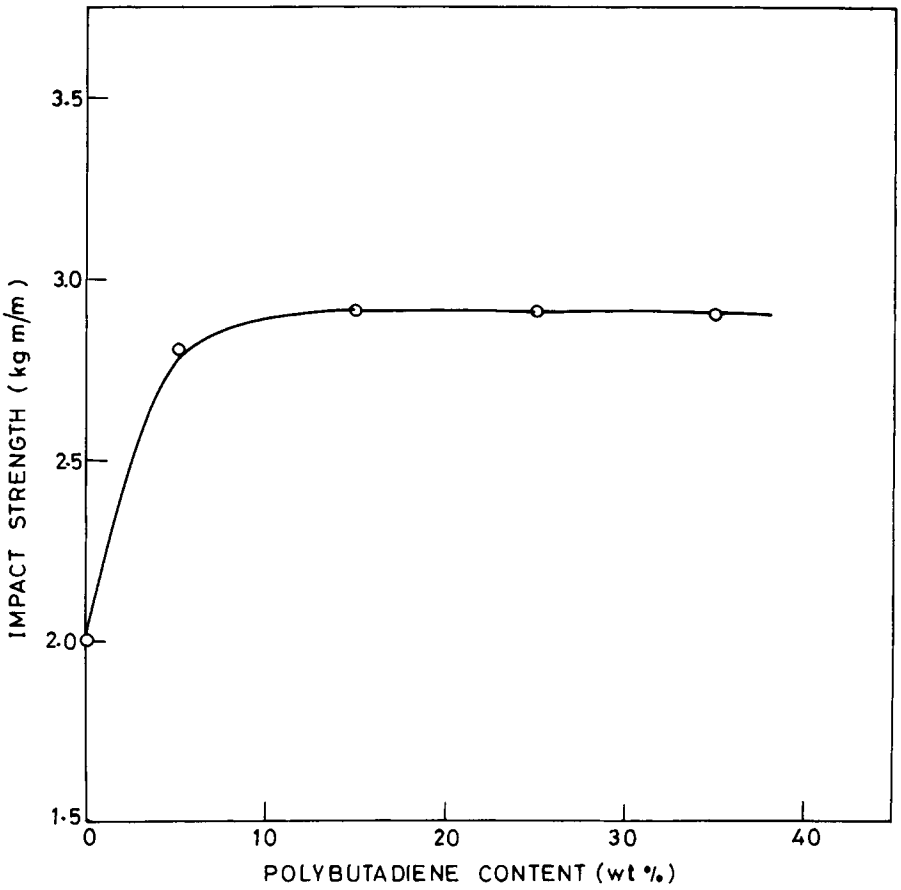

Figure 5 Izod impact strength of notched samples as a function of PBu content for PP/PBu blend.

at 5% PBu content is higher than that of unblended PP. The trends of variation of X-ray and DSC crystallinities are similar at low PBu content and differ only at high PBu content. A possible reason for this disparity is that the calculation of X-ray crystallinity was based on a method appropriate for pure PP and not for the blend, where the contribution of amorphous scattering of the second component (PBu in the present case) might become appreciable, more so at high proportion of the second component.

Crystallite size was calculated by Scherrer's equation[20]

$$t_{hkl} = \frac{0.89\lambda}{B \cos \theta_{hkl}}, \qquad (1)$$

where t_{hkl} is crystallite dimension perpendicular to the lattice plane (hkl), λ is wavelength of X-rays, B is width at half-height of the diffraction maximum, and θ_{hkl} is the Bragg angle corresponding to the hkl plane. The crystallite size in the direction perpendicular to the (110) plane shows no significant variation, while the crystallite size corresponding to the (040) lattice plane increases with increasing PBu content of the blend, as shown in Table I. The ratio t_{040}/t_{110} of these two crystallite sizes distinctly increases with increasing PBu content.

Mo et al.[21] studied in detail the effect of blending and copolymerization on the X-ray diffraction pattern of PP and reported two important observations: (i) the appearance of an extra reflection around $2\theta = 20°$ due to the formation of γ-crystalline form of PP and (ii) the increase of intensity of (040) reflection accompanied by no change or a decrease of intensity of (110) reflection. Effect (i) is absent in these data, whereas effect (ii) is quite distinct, as shown in Table I, where the ratio I_{040}/I_{110} of intensities of (040) reflection to that of (110) reflection increases continuously with increasing PBu content of the blend. This finding supports Mo et al.'s[21] contention that I_{040}/I_{110} increases on blending the PP whereas the formation of γ-crystalline modification is favored on copolymerization. The increase in the

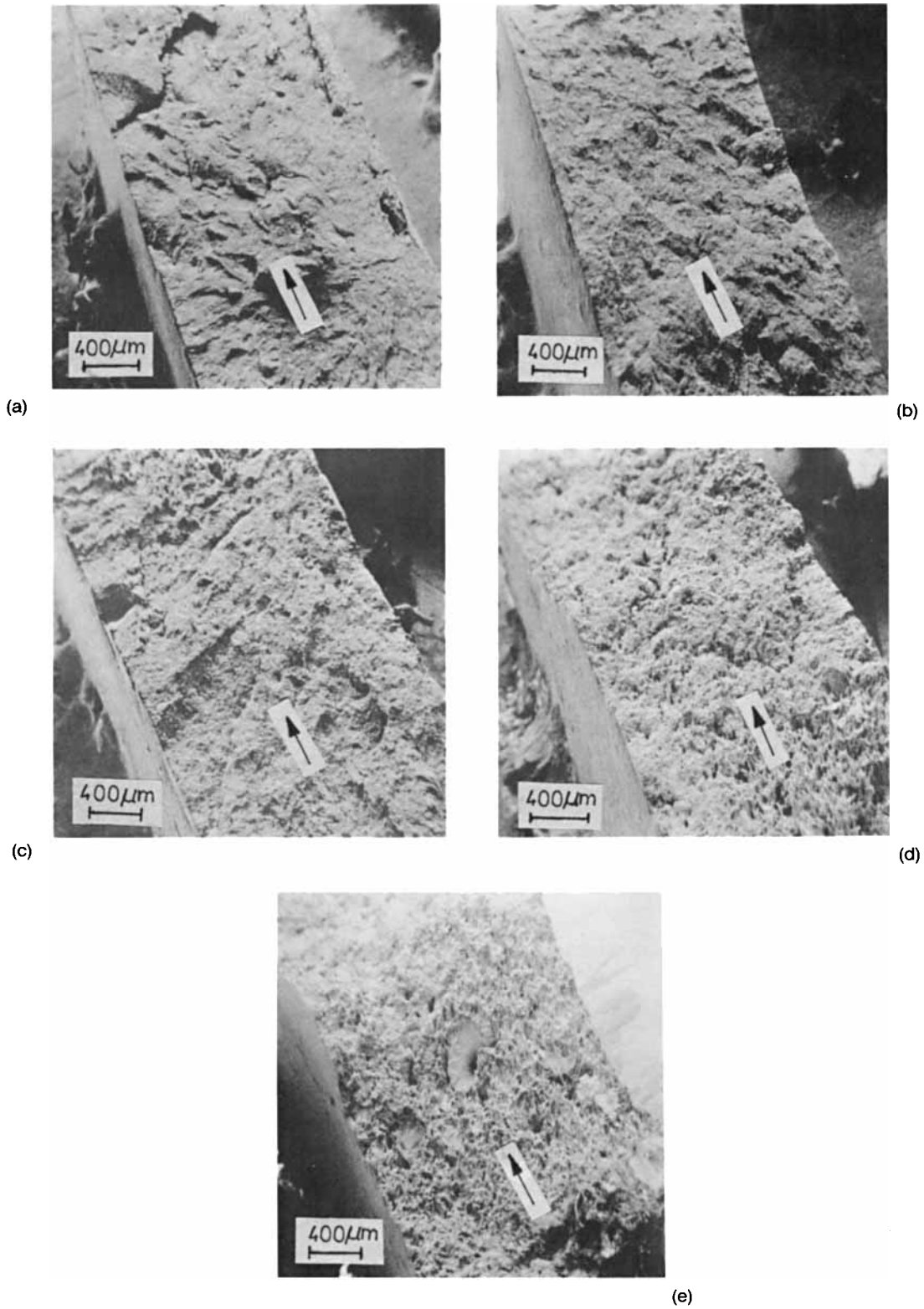

Figure 6 SEMs at low magnification, of impact-fractured surfaces of PP/PBu blend at various PBu contents (wt %): (a), 0; (b), 5; (c), 15; (d), 25; (e), 35. Arrow indicates the direction of applied stress.

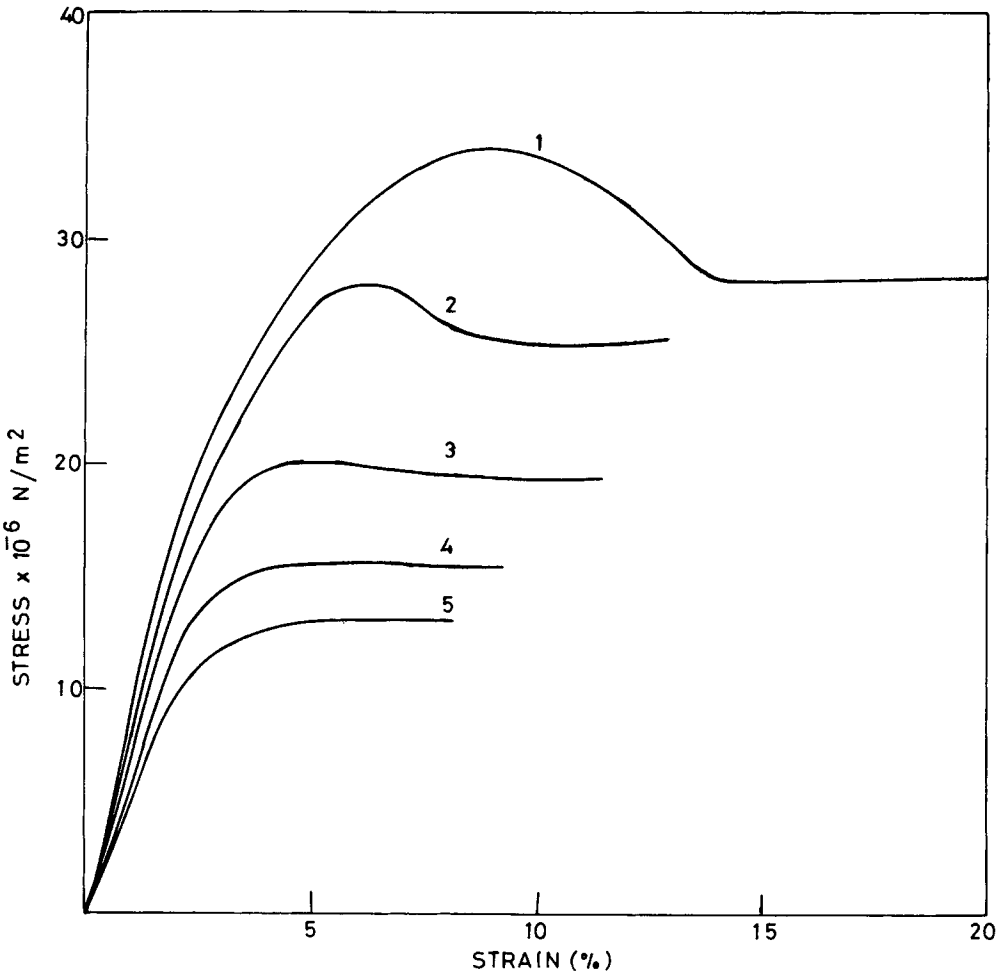

Figure 7 Tensile stress–strain curves in yield region of PP/PBu blend at various PBu contents (wt %): (1), 0; (2) 5; (3), 15; (4), 25; (5), 35.

ratio of intensities I_{040}/I_{110} implies that the growth of crystallites is more in the direction perpendicular to (040) plane than the direction perpendicular to (110) plane, as also interpreted by Mo et al.[21] Variation of crystallite size calculated from these diffraction maxima, shown in Table I, supports this. Such an effect was observed earlier on a PP/SEBS blend[2] but could not be emphasized until the explanation came from Mo et al.[21]

Impact Properties

Variation of izod impact strength of notched samples with blend composition is shown in Figure 5. The impact strength of PP increases by a factor of 1.5 on the initial addition of 5 wt % PBu and thereafter remains constant at this higher value in the entire studied range of PBu content. Hence, for the purpose of impact strength improvement of PP by blending with PBu, only the smaller PBu content (i.e., 5 wt %) is good enough. Smaller PBu content is preferable from the point of view of smaller deterioration of tensile and other mechanical properties since the greater the elastomer content the greater will be the deterioration in tensile strength and modulus.

An examination of scanning electron micrographs of impact fractured samples, presented in Figure 6, shows a variation in the mode of fracture with increasing PBu content of the blend. The brittle fracture observed at 0% PBu content changes gradually to ductile fracture with increasing PBu content. Uprooting of some PBu droplets is also seen in the fracture surface micrographs of unetched samples, which indicates their poor adhesion with PP matrix. The features characteristic of shear yielding, viz. lateral contraction and striations at an angle 30–60° with the direction of applied stress, are present in all these fracture surfaces. The features of ductile

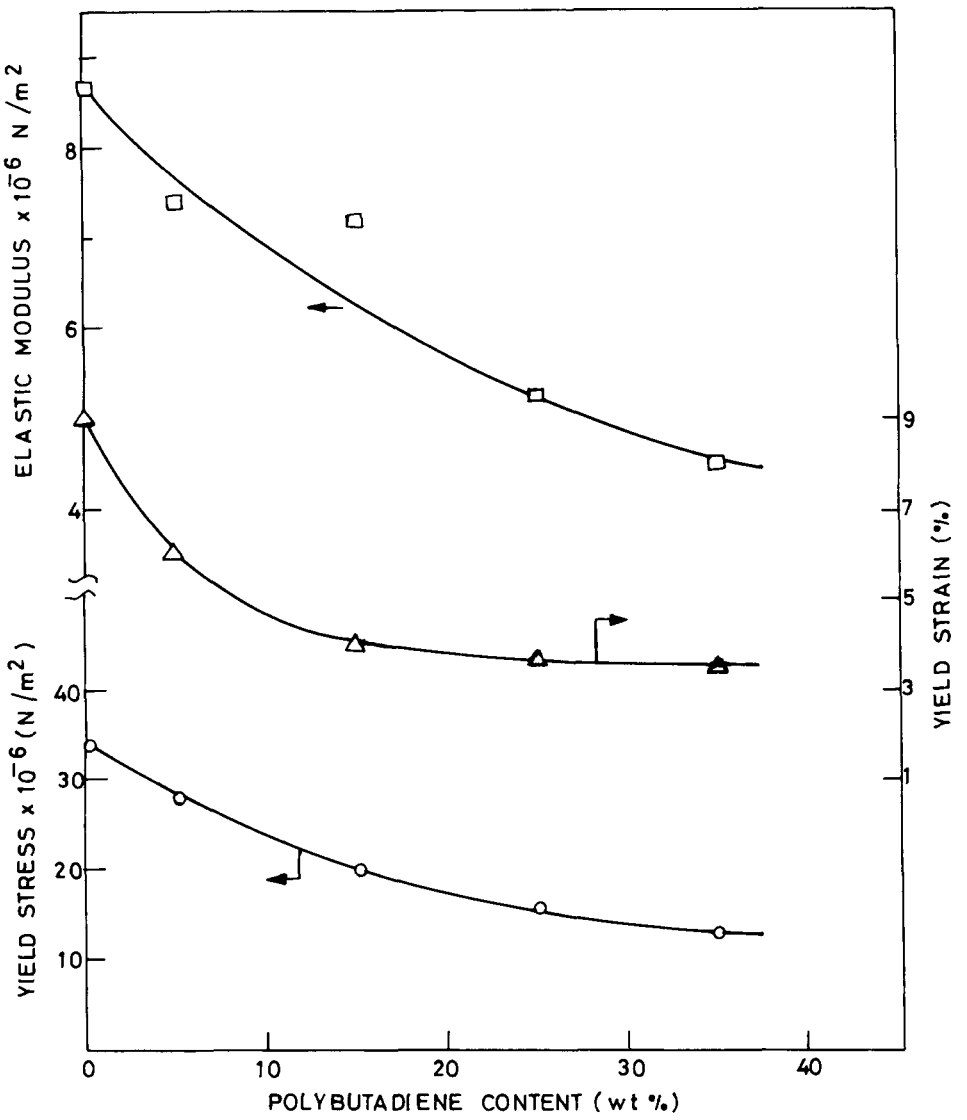

Figure 8 Variations of yield stress, yield strain, and elastic modulus with PBu content for PP/PBu blend.

fracture and shear yielding were also observed in PP/SEBS[6] and PP/ABS[22] blends.

Tensile Properties

The stress–strain curves in the yield region of PP/PBu blends at various compositions and the unblended PP are shown in Figure 7. Stress rises with strain first quite sharply and then gradually and finally shows a slight decrease after passing through the yield point. PP shows a peak in the yield region at around 8–10% strain, and the yield stress (i.e., the highest stress reached just before yielding) is 3.4×10^7 N/m^2. On addition of PBu, the yielding process seems to undergo changes such that the yield peak disappears at high PBu content. At 5 wt % PBu content, a narrow yield peak at yield stress 2.8×10^7 N/m^2 is observed. On further increase of PBu content, the yield peak disappears and the stress–strain curve flattens to a shape similar to that of elastomers. The yield stress and yield strain in such cases is determined from the turning point of the curve, established from the intersection of tangents on the relevant portions. The yield stress and yield strain thus determined are shown in Figure 8 as functions of the blend composition. Also shown in the figure are the values of elastic modulus corresponding to the initial linear portion of the stress–strain curves. Elastic modulus of the blend decreases with increasing PBu content. However, at 5 wt %

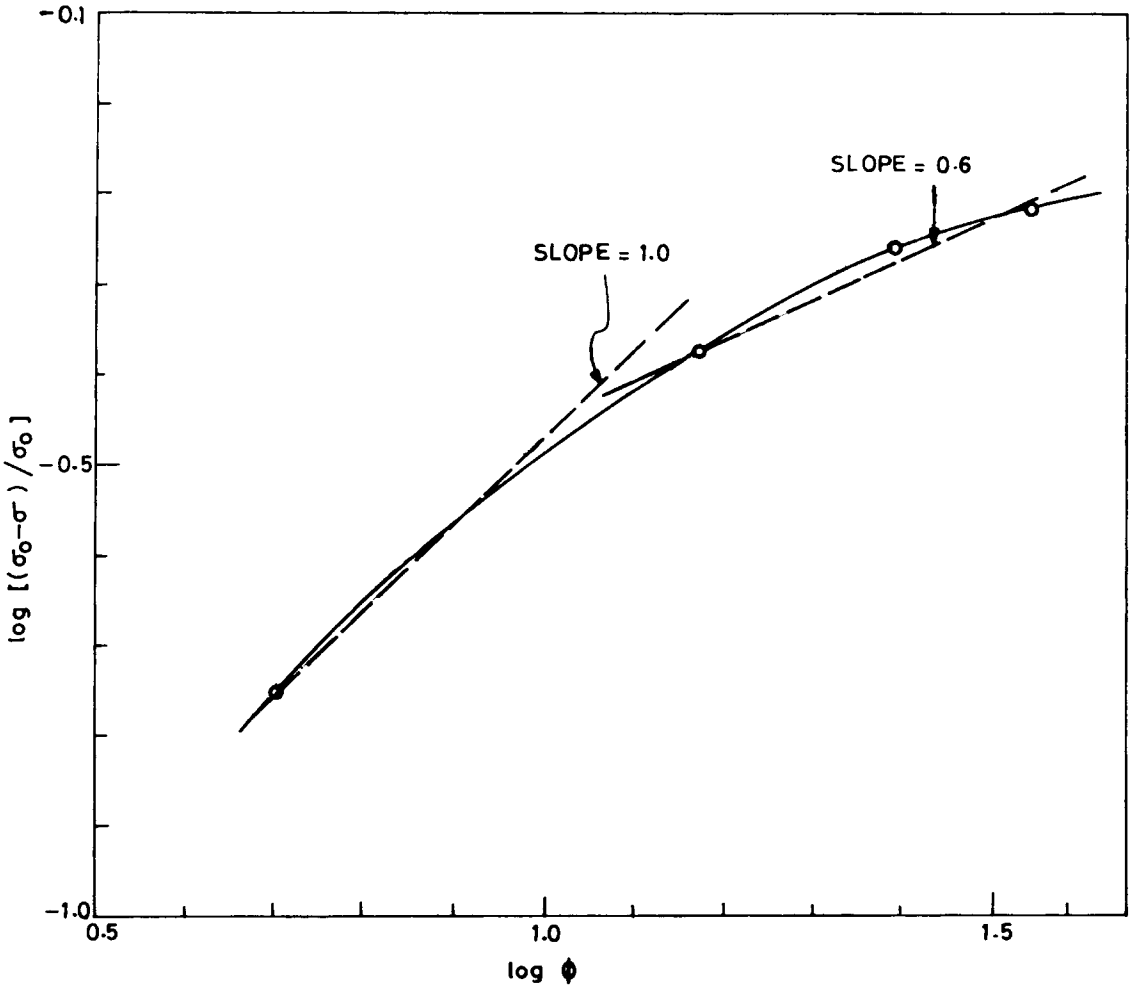

Figure 9 Variation of log $[(\sigma_0 - \sigma)/\sigma_0]$ with log ϕ for PP/PBu blend and its comparison with the limiting slopes at the two extremes.

PBu content, i.e., the case for which impact strength improvement was maximum, the decrease of yield stress and modulus is only about 15%. This may prove to be a useful combination of the two properties to suit various end-use applications.

Analysis for Discontinuities in Stress Transfer

Analysis of variation of mechanical properties with blend composition in terms of the theoretical models provides knowledge about discontinuities in stress transfer in two-phase blends, as described below.

Exponent of the Power Law

The two most common expressions for composition dependence of mechanical properties of the two-phase blends (or composites) are based on the "first-power" law and "two-thirds power" law, stated below:

$$\sigma = \sigma_0(1 - \phi) \tag{2}$$

$$\sigma = \sigma_0(1 - \phi^{2/3}), \tag{3}$$

where σ and σ_0 denote the mechanical property of the blend and of the matrix (i.e., the major component of the blend), respectively, and ϕ is the volume fraction of the inclusion (i.e., the dispersed phase). These power laws originate from the considerations of the effect of area fraction and volume fraction of the inclusions in the modification of the property.[23,24] For a completely random distribution of the dispersed phase, the first-power relationship of area fraction to volume fraction in any randomly chosen plane of fracture is derived.[24] On the other

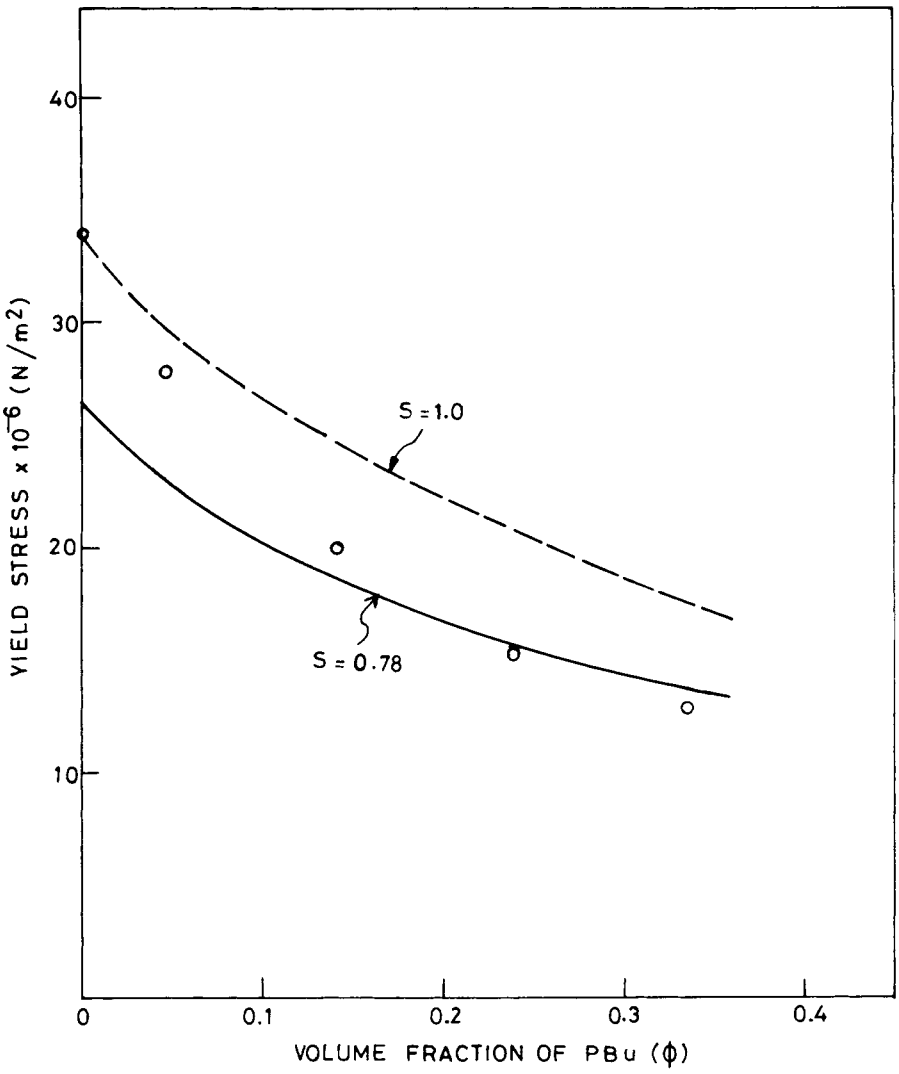

Figure 10 Yield stress data as a function of volume fraction of PBu for PP/PBu blend, and the theoretical curves according to eq. (4) for two values of S, discussed in the text.

hand, for the case of spherical inclusions the two-thirds power law with appropriate weightage factor is derived.[24] It is, however, difficult to say which of these two laws should hold for a given system. This uncertainty is emphasized through experimental evidence by Kunori and Geil[23] based on the analyses of SEM pictures of fracture surfaces of two-phase blends.

Validity of both power laws is seen for this blend in different ranges of blend composition. The plot $\log [(\sigma_0 - \sigma)/\sigma_0]$ vs. $\log \phi$ (Fig. 9) shows a curvature, implying a change of slope. The slope, which is equal to the exponent of ϕ in eq. (2) and (3), changes from 0.6 (at high values of ϕ) to unity (at low values of ϕ). This shows that the power law exponent changes from unity to two-thirds with increasing PBu content of the blend. Kunori and Geil[23] also emphasized the composition dependence of the validity of both first-power and two-thirds power laws and attributed it to shape of the inclusions. The shape of the inclusion, as will be described in a subsequent section, changes from spherical at low PBu content to nonspherical at high PBu content in these blends.

Stress Concentration Parameters

A further modification in the two-thirds power law expression, reported by Nielsen,[25] incorporates a

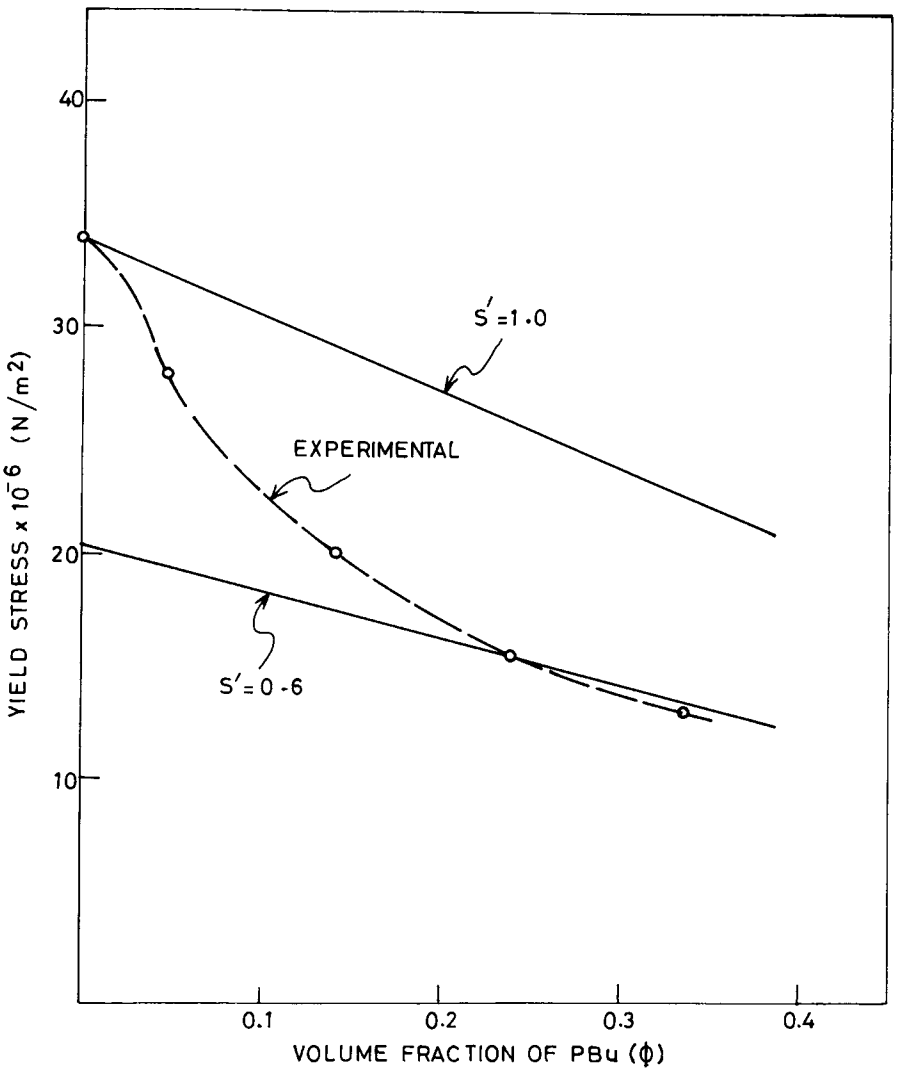

Figure 11 Sigmoidal transition curve (broken time) passing through the experimental data for PP/PBu blend and the theoretical lines according to eq. (5) with the $S' = 1$ and 0.6, coinciding with the two extremes of the sigmoidal transition curve.

parameter S to take into account the stress concentration effect. Nielsen's equation is as follows:

$$\sigma = \sigma_0(1 - \phi^{2/3})S. \qquad (4)$$

S is unity when the stress transfer is continuous and $S < 1$ implies the occurrence of stress concentration. Theoretical variation according to the "unmodified two-thirds power law" [i.e., eq. (4) with $S = 1$], shown by the broken curve in Figure 10, represents the decrease of yield stress due to the presence of the second phase. On the other hand, the "modified two-thirds power law" with $S = 0.78$ (solid curve in Fig. 10) includes the additional effect of stress concentration. Thus, the result of the stress concentration effect is to shift the σ vs. ϕ curve downward. The experimental data that points at high values of ϕ are in perfect agreement with this theoretical curve for $S = 0.78$, whereas at low values of ϕ the data points deviate systematically from this theoretical curve. This indicates that the stress concentration effect is predominant at high-volume fractions of the second phase. Incidentally, this occurrence of the stress concentration effect at high PBu content in this blend is consistent with the large size of the PBu droplets, as will be described in a later section.

A similar modification of the first-power law by incorporating a stress concentration factor S' (which may differ from S of eq. (4), proposed by Gupta and

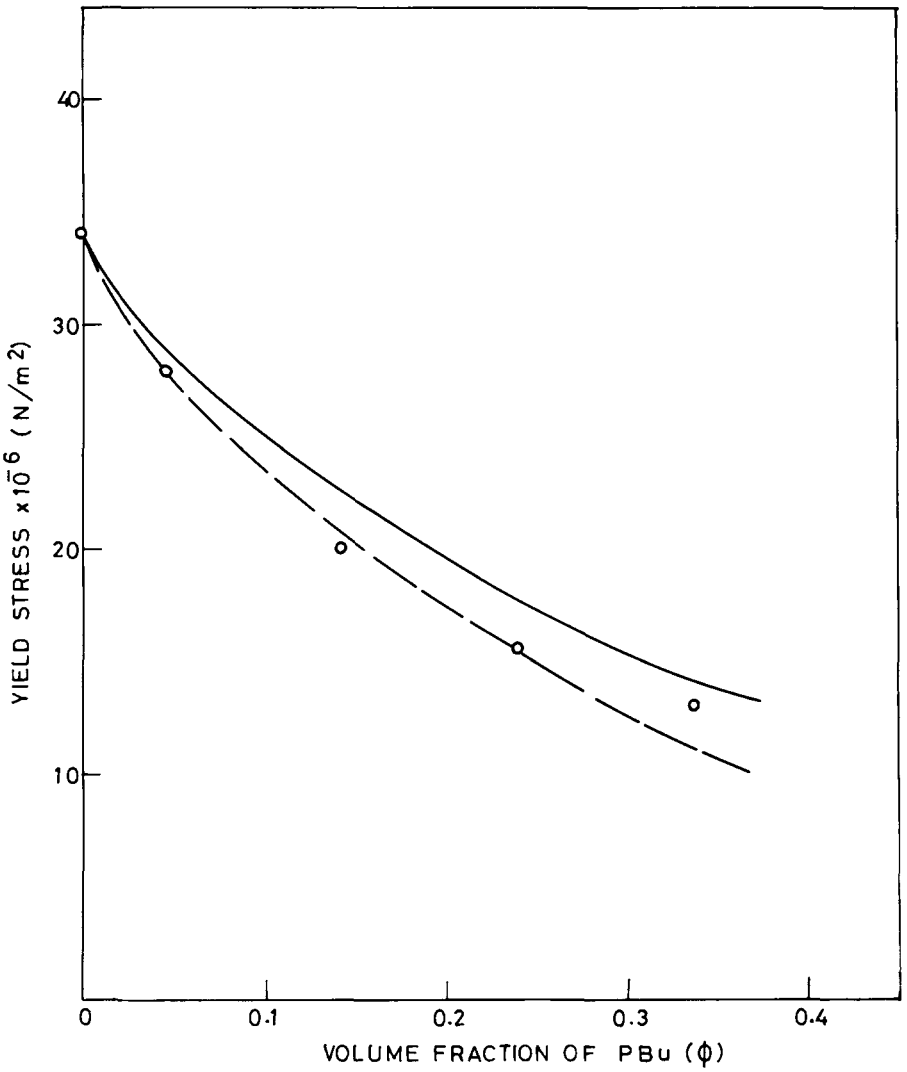

Figure 12 Theoretical curves according to eq. (6) with two values of the weightage factor 1.21 (solid line) and 1.40 (broken line) and the experimental data points for PP/PBu blend.

Purwar,[3] leads to the following expression for the variation of yield stress of the blend:

$$\sigma = \sigma_0(1 - \phi)S', \tag{5}$$

where $S' = 1$ in the absence of stress concentration and $S' < 1$ in the presence of stress concentration. The experimental data fall between the two extremes represented by theoretical variations of eq. (5) for $S = 1$ and $S = 0.6$, shown by solid lines in Figure 11. The data points seem nicely represented by a sigmoidal transition curve (broken curve in Fig. 11) coinciding with the respective theoretical curves at its two extremes. Such sigmoidal transitions from a state of low-stress concentration to a state of high-stress concentration are also observed in other two-phase blends.[3]

Nicolais and Narkis[26] suggested the incorporation of a weightage factor of 1.21 in the expression of the two-thirds power law as follows:

$$\sigma = \sigma_0(1 - 1.21\phi^{2/3}). \tag{6}$$

The parameter 1.21 in eq. (6), viewed by some authors[23] as a parameter equivalent to the stress concentration parameter S of Nielsen, has been shown by Piggott and Leidner[24] to be the outcome of the spherical shape of the inclusions. Hence, for the case of nonspherical droplets of the inclusion eq. (6) may be modified using the weightage factor

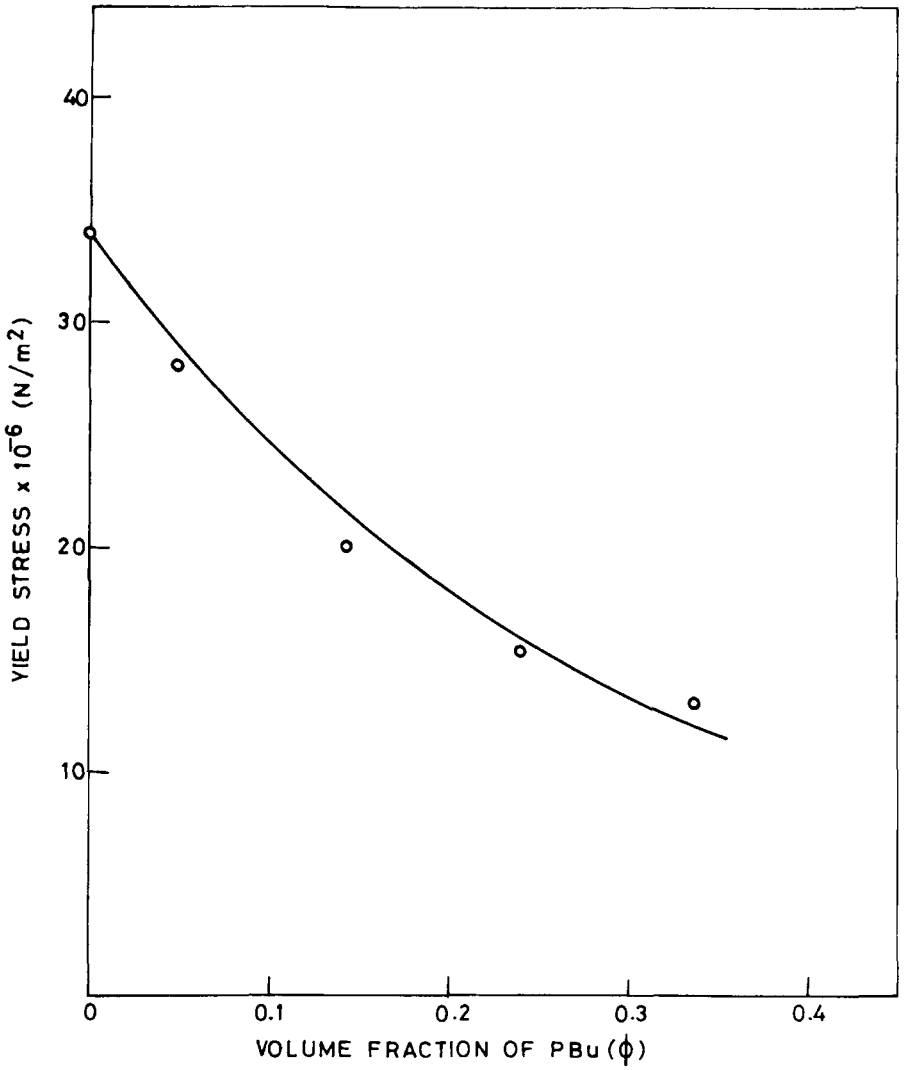

Figure 13 Theoretical curve according to eq. (8) for **a** = 3.1 with experimental data for PP/PBu blend.

greater than 1.21. Figure 12 shows the two theoretical variations of eq. (6) with weightage factors 1.21 and 1.40. The experimental data fall closer to the theoretical curve with weightage factor 1.40, suggesting greater stress concentration than what is accommodated in Nicolais and Narkis' equation for spherical droplets of the dispersed phase.

Porosity Model

A porosity model, which was found by Nielsen[27] applicable to a polymer matrix with voids and holes and by Kunori and Geil[23] to polymer blends with poor adhesion, was also used in the analysis of these results. According to the porosity theory, the specific change $d\sigma/\sigma$ in a property is directly proportional to the porosity P or

$$\frac{d\sigma}{\sigma} = -\mathbf{a}P, \tag{7}$$

where **a** is proportionality constant and a negative sign implies the mutually opposite sense of variation of σ and P. Replacing the total porosity with volume fraction ϕ of the inclusion, the expression for two-phase blend may be written as

$$\sigma = \sigma_0 \exp(-\mathbf{a}\phi). \tag{8}$$

The relationship of the parameter **a** and the stress concentration effect has been suggested[23] such that the higher the stress concentration the higher the value of **a**. The present data show good agreement with the porosity model expression with one single

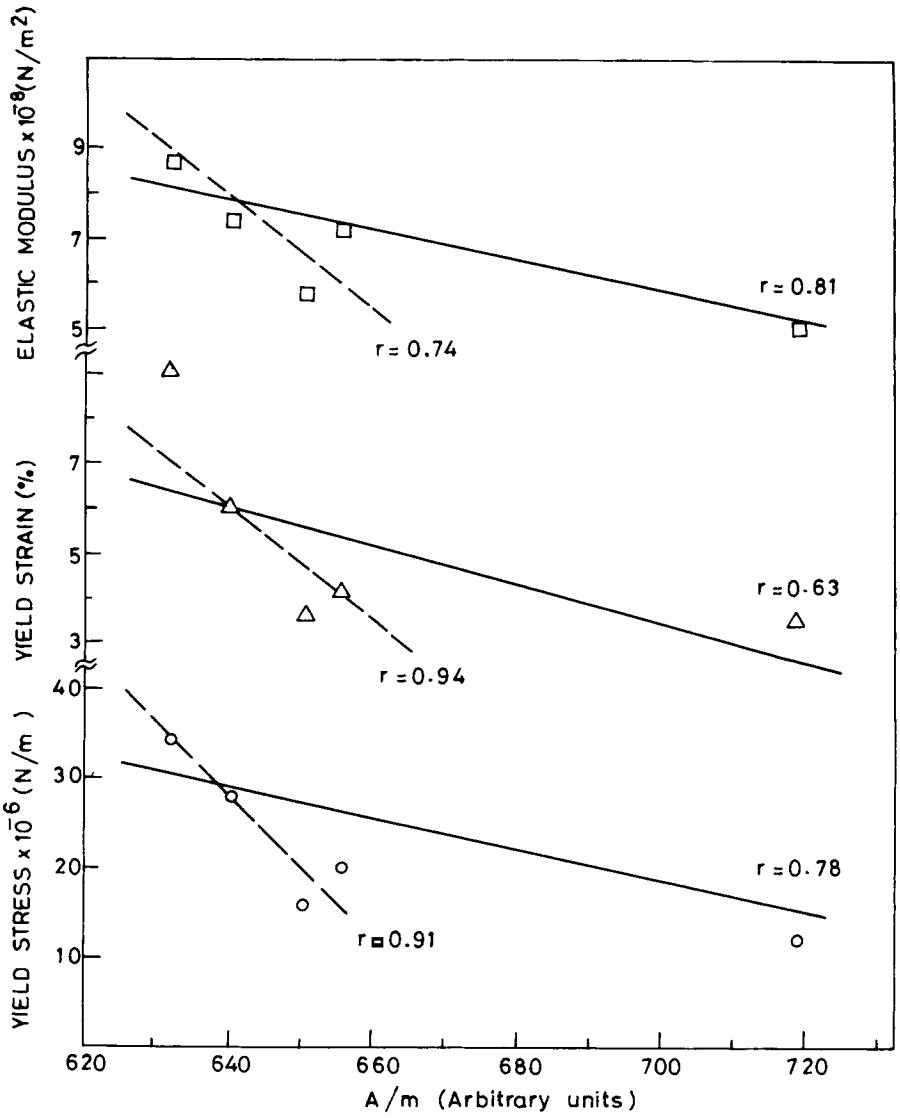

Figure 14 Variation of tensile properties with DSC crystallinity parameter A/m for PP/PBu blend. The best-fitting straight lines and their coefficients of correlation (r) are shown for: (i) all five data points (solid line); and (ii) four data points excluding the outlying one point (broken line).

value of the parameter **a** = 3.1 over the entire range of the blend composition studied, as shown in Figure 13. This value of **a** is rather high as compared to the values obtained (viz., 1.7–2.6) for PP/SEBS blend,[3] implying the superiority of SEBS copolymer over PBu for blending with PP.

These analyses based on the various theoretical models lead to identical conclusions and hence strengthen our belief in them. With increase of PBu content in the PP/PBu blend, the discontinuities in stress transfer increase. This may be attributed to the formation of dispersed phase droplets of non-spherical shapes with sharp corners that provide the sites for stress concentration. This is supported by the existence of irregularly shaped PBu droplets at higher PBu content in the blend, as seen in the SEM photographs presented in a subsequent section.

Correlation of Tensile Properties and Crystallization

Crystallization affects the mechanical properties of all polymers. However, the effect of individual crystallization parameters such as degree of crystallinity and crystallite size distribution may have different effects on different mechanical properties. We have,

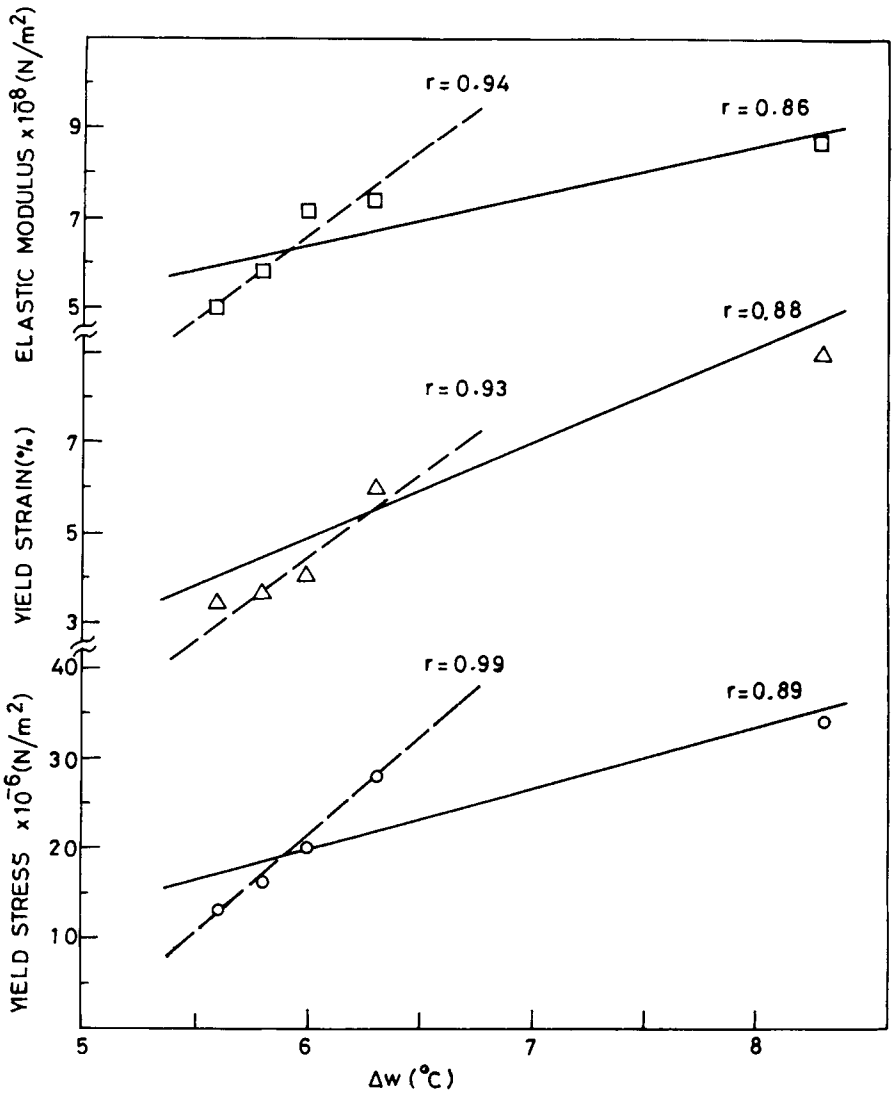

Figure 15 Variation of tensile properties with DSC crystal size distribution parameter Δw for PP/PBu blend. The best-fitting straight lines and their coefficients of correlation are shown for (i) all five data points (solid line) and (ii) four data points excluding the outlying one point (broken line).

therefore, examined the correlation of these two crystallization parameters with the tensile properties viz. elastic modulus, yield stress, and yield strain. The two crystallization parameters in this analysis are Δw, related to crystallite size distribution, and A/m, related to degree of crystallinity determined from DSC crystallization exotherms. The coefficient of correlation was determined by regression analysis. Data on all five samples and their best-fitting linear extrapolations (solid lines) are shown in Figures 14 and 15 with the coefficients of correlation (r). The correlations are better in the case of the parameter Δw than A/m, as seen from the values of r. However, in these data (Figs. 14 and 15) there is an outlying point in each correlation that tends to force the line to pass through it. Hence, the value of r might be influenced by this tendency. The correlations obtained after excluding the outlying point are shown by broken lines in Figures 14 and 15 with their respective values of r. These latter correlations are somewhat better as indicated by their values of r, except in the case of yield strain vs. Δw.

This linear correlation of the tensile properties with crystallization parameters of PP indicates that the crystallization of the matrix plays a significant role in the tensile behavior of the PP/PBu blend.

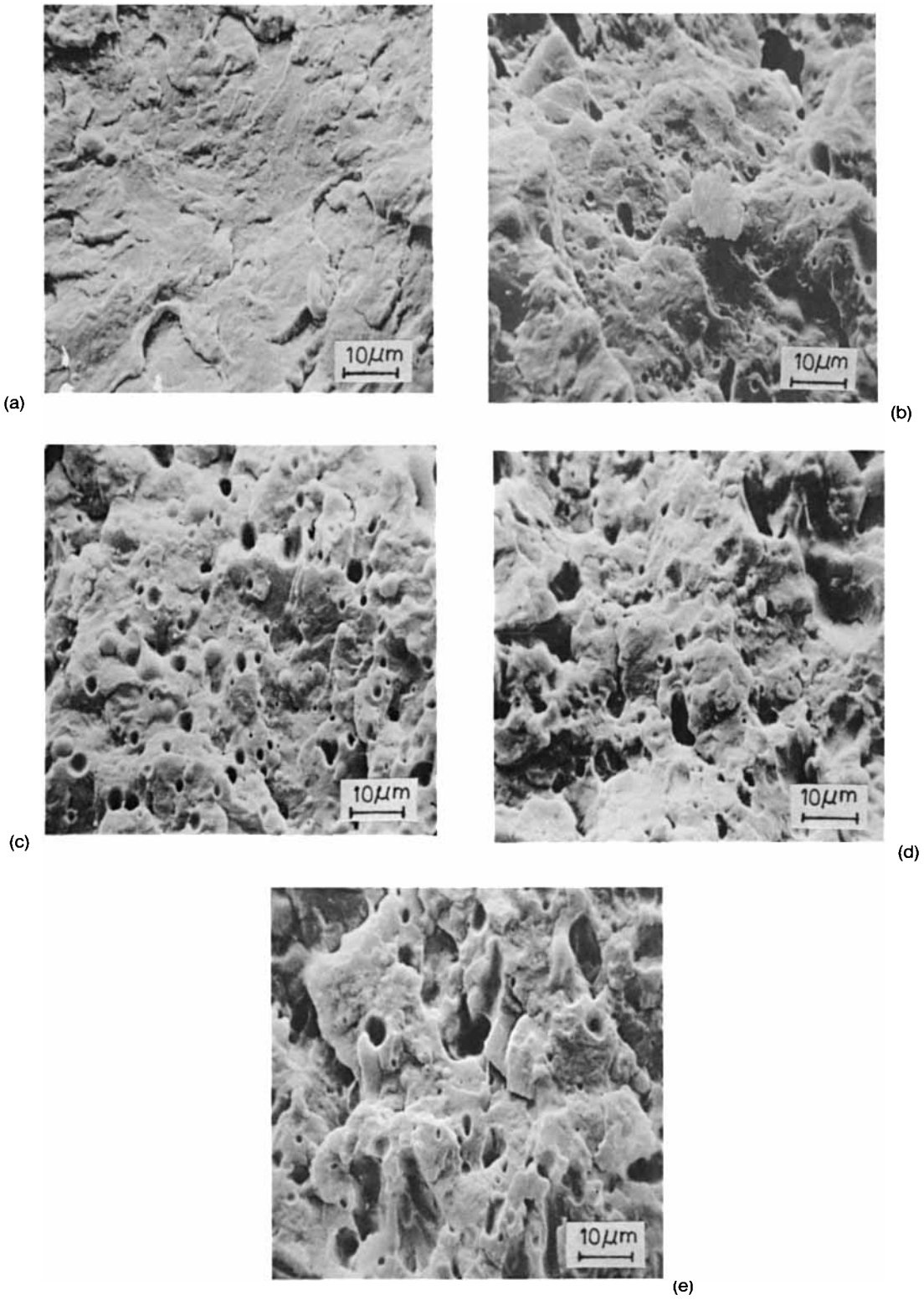

Figure 16 SEMs of fracture surfaces at high magnification to illustrate the state of dispersion of the PP/PBu blend at various PBu contents (wt %): (a), 0; (b), 5; (c), 15; (d), 25; (e), 35.

Furthermore, as seen from these plots, the correlations with Δw are good for most of the mechanical properties (yield stress, yield strain, and elastic modulus). This indicates that crystallite size distribution plays a role in tensile properties. Hence, it may be emphasized that for describing the effect of crystallization on mechanical properties, the crystallite size distribution must be given due importance in addition to crystallinity.

State of Dispersion

The SEMs of the impact fractured and etched surfaces of PP/PBu blend at various compositions are shown in Figure 16. The voids in these micrographs represent the spaces left behind by the PBu droplets. Although there is a considerable distribution of droplet size, it is clearly apparent that the average size of the droplet is smallest at 5 wt % PBu content and increases with increasing PBu content. The droplets are sufficiently spherical at low PBu content [see Figs. 16(b) and (c)] and somewhat nonspherical at higher PBu content [see Figs. 16(d) and (e)]. The mean diameters (determined by measuring the diameters on at least 20 droplets in each micrograph) of the PBu droplets were 1.5, 3, 4, and 6 μm for 5, 15, 25, and 35 wt % PBu content, respectively. The large size and nonspherical shape of the dispersed phase droplets at high PBu content are quite consistent with their role in the discontinuities of stress transfer (or stress concentration effect) found in the theoretical analysis of tensile properties (see Analysis for Discontinuities in Stress Transfer) of this blend at high PBu contents.

CONCLUSION

A blend of PP and PBu prepared by mixing in a roll-mill forms a two-phase morphology with good dispersion of PBu droplets. At identical conditions of mixing, the mean diameter of the dispersed droplets increases with increasing PBu content. Unlike several other elastomers, PBu forms quite round (spherical or elliptical) droplets in PP matrix.

Crystallization of PP is affected by the presence of PBu, such that the rates of nucleation and crystallinity are higher in the blend than in PP. With varying PBu content, changes in crystallization behavior, attributable to the morphology of dispersed phase, are also observed.

Crystallite size in (040) direction increases on addition of PBu, while that in the (110) direction shows little variation. Such an effect, observed previously on other blends of PP,[2] went unemphasized until the publication of its origin.[21]

Impact strength of PP improves by a factor of 1.5, and 5 wt % PBu addition is sufficient for this. At this composition of the blend, loss of tensile properties is small (about 15% decrease in yield stress). This combination of properties may suit various end uses and thus enhance the scope of application of PP.

Tensile properties deteriorate with increasing PBu content of the blend. Theoretical analysis of yield stress data reveals that discontinuities in stress transfer due to stress concentration become appreciable when PBu content exceeds 15 wt %. SEM shows changes in shape and size of PBu droplets with increasing PBu content that are conducive to stress concentration effect.

REFERENCES

1. A. K. Gupta and S. N. Purwar, *J. Appl. Polym. Sci.*, **29,** 1079 (1984).
2. A. K. Gupta and S. N. Purwar, *J. Appl. Polym. Sci.*, **29,** 1595 (1984).
3. A. K. Gupta and S. N. Purwar, *J. Appl. Polym. Sci.*, **29,** 3513 (1984).
4. A. K. Gupta and S. N. Purwar, *J. Appl. Polym. Sci.*, **30,** 1777 (1985).
5. A. K. Gupta and S. N. Purwar, *J. Appl. Polym. Sci.*, **30,** 1799 (1985).
6. A. K. Gupta and S. N. Purwar, *J. Appl. Polym. Sci.*, **31,** 535 (1986).
7. F. C. Stehling, T. Huff, C. S. Speed, and G. Wissler, *J. Appl. Polym. Sci.*, **26,** 2693 (1981).
8. W. J. Ho and R. Salovy, *Polym. Eng. Sci.*, **21,** 839 (1981).
9. L. D'Oragio, R. Greco, C. Manearella, E. Martuscelli, G. Ragosta, and C. Silvestre, *Polym. Eng. Sci.*, **22,** 536 (1982).
10. L. D'Oragio, R. Greco, E. Martuscelli, and G. Ragosta, *Polym. Eng. Sci.*, **23,** 489 (1983).
11. I. Duvdevani, P. K. Agarwal, and R. D. Lundberg, *Polym. Eng. Sci.*, **22,** 499 (1982).
12. S. Danesi and R. S. Porter, *Polymer*, **19,** 448 (1978).
13. P. Galli, S. Danesi, and T. Simonazzi, *Polym. Eng. Sci.*, **24,** 544 (1984).
14. J. Ito, K. Mitani, and Y. Mizutani, *J. Appl. Polym. Sci.*, **29,** 75 (1984).
15. D. Yang, B. Zhang, Y. Yang, Z. Fang, G. Sun, and Z. Feng, *Polym. Eng. Sci.*, **24,** 612 (1984).

16. W. Y. Chiu and S. J. Fang, *J. Appl. Polym. Sci.*, **30,** 1473 (1985).
17. R. Greco, G. Manearella, E. Martuscelli, G. Ragosta, and Y. Jinghua, *Polymer,* **28,** 1929 (1987).
18. A. K. Gupta, V. B. Gupta, R. H. Peters, W. G. Harland, and J. P. Berry *J. Appl. Polym. Sci.*, **27,** 4669 (1982).
19. G. Guerra, V. Pettraccone, P. Corradini, C. De Rosa, R. Napolitano, and B. Pirrozo, *J. Polym. Sci. Polym. Phys. Ed.*, **22,** 1029 (1984).
20. H. P. Klug and L. E. Alexander, *X-ray Diffraction Procedure for Crystalline & Amorphous Materials,* Wiley, New York (1967), Chap. 9.
21. Z. Mo, L. Wang, H. Zhang, P. Han, and B. Huang, *J. Polym. Sci. Polym. Phys. Eds.*, **25,** 1829 (1987).
22. A. K. Gupta, A. K. Jain, B. K. Ratnam, and S. N. Maiti, *J. Appl. Polym. Sci.*, **39,** 515 (1990).
23. T. Kunori and P. H. Geil, *J. Macromol. Sci. Phys.*, **B-18,** 135 (1980).
24. M. R. Piggott and J. Leidner, *J. Appl. Polym. Sci.*, **18,** 1619 (1974).
25. L. E. Nielsen, *J. Appl. Polym. Sci.*, **10,** 97 (1966).
26. L. Nicolais and M. Narkis, *Polym. Eng. Sci.*, **11,** 194 (1971).
27. L. E. Nielsen, *J. Compos. Mater.*, **1,** 100 (1967).

Accepted January 29, 1990